

Article

# Transformative Si<sub>8</sub>R<sub>8</sub> Siliconoids

Naohiko Akasaka, Shintaro Ishida  and Takeaki Iwamoto \*Department of Chemistry, Graduate School of Science, Tohoku University, Sendai 980-8578, Japan;  
nao.akasaka1216@gmail.com (N.A.); ishida@tohoku.ac.jp (S.I.)

\* Correspondence: takeaki.iwamoto@tohoku.ac.jp; Tel.: +81-22-795-6558

Received: 3 September 2018; Accepted: 1 October 2018; Published: 3 October 2018



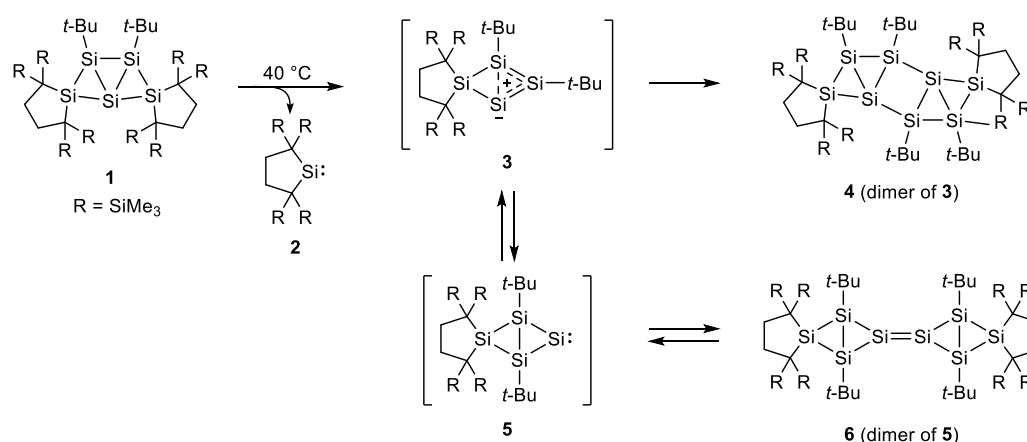
**Abstract:** Molecular silicon clusters with unsubstituted silicon vertices (siliconoids) have received attention as unsaturated silicon clusters and potential intermediates in the gas-phase deposition of elemental silicon. Investigation of behaviors of the siliconoids could contribute to the greater understanding of the transformation of silicon clusters as found in the chemical vapor deposition of elemental silicon. Herein we reported drastic transformation of a Si<sub>8</sub>R<sub>8</sub> siliconoid to three novel silicon clusters under mild thermal conditions. Molecular structures of the obtained new clusters were determined by XRD analyses. Two clusters are siliconoids that have unsaturated silicon vertices adopting unusual geometries, and another one is a bis(disilene) which has two silicon–silicon double bonds interacted to each other through the central polyhedral silicon skeleton. The observed drastic transformation of silicon frameworks suggests that unsaturated molecular silicon clusters have a great potential to provide various molecular silicon clusters bearing unprecedented structures and properties.

**Keywords:** cluster; isomerization; silicon; siliconoid; subvalent compounds

## 1. Introduction

Molecular silicon clusters have attracted much attention as their characteristic electronic properties and reactivity depend on the structures [1–5]. In the chemical vapor deposition (CVD) process of elemental silicon, unsaturated silicon clusters with unsubstituted silicon vertices are considered as potential intermediates [6–8]. Recently, such kinds of unsaturated molecular silicon clusters are synthesized as isolable molecules [9–22] and termed “siliconoids” by Scheschkewitz et al. [10]. The siliconoids show their characteristic distorted structures and large distribution of <sup>29</sup>Si nuclear magnetic resonances. As the unsubstituted vertices are considered to be preferred reaction sites for transformation of silicon clusters [23–25], investigation of thermal transformation of the siliconoids would provide fundamental reactions that may contribute to improving our understanding of the mechanism of the CVD process elemental silicon [26–30]. However, thermal transformation of siliconoids is still scarce. Scheschkewitz et al. have reported thermal rearrangement, expansion, and contraction of Si<sub>6</sub>Tip<sub>6</sub> (Tip = 2,4,6-triisopropylphenyl) siliconoids [10,13,15–17,22].

Recently, we reported that thermal reaction of Si<sub>5</sub>R<sub>6</sub> siliconoid **1** at 40 °C afforded Si<sub>8</sub>R<sub>8</sub> siliconoids **4** and **6**, the latter of which undergoes thermal isomerization to **4** upon extra heating (Scheme 1). In this transformation, elimination of a silylene unit (SiR<sub>2</sub>, **2**) from **1** generates disilene **3** and silylene **5**, which equilibrate with each other and dimerize to give **4** and **6**, respectively [22]. As **4** has still highly strained structures similar to **1**, we examined further thermal reactions of **4**. Herein, we report thermal transformation of **4** giving new silicon clusters that involve highly distorted silicon atoms, silicon–silicon double bonds, or unsubstituted silicon vertices. The observed drastic transformation suggests that unsaturated molecular silicon clusters have a great potential to provide various molecular silicon clusters bearing unprecedented structures and properties.

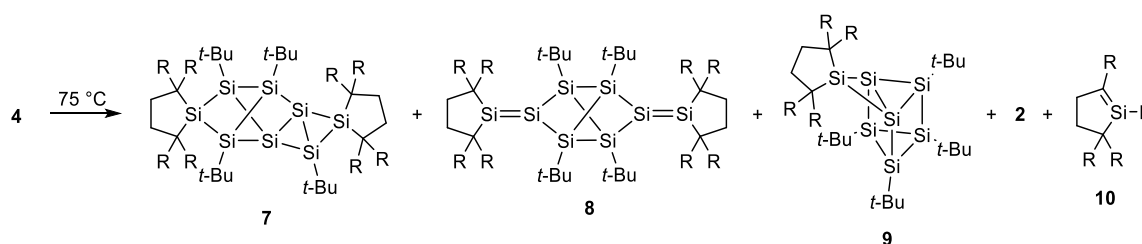


**Scheme 1.** Thermal transformation of 1. R = SiMe<sub>3</sub>.

## 2. Results

### 2.1. Thermal Reactions of 4

Upon heating 4 at 75 °C in benzene-*d*<sub>6</sub>, new silicon clusters with unprecedented silicon frameworks 7, 8, and 9 were formed together with silylene 2 and its thermal isomerization product, silene 10 (Scheme 2). Compounds 7 and 8 are isomers of 4 and 6 bearing the formula of Si<sub>8</sub>R<sub>8</sub>, while 9 is a contracted Si<sub>7</sub>R<sub>6</sub> cluster. Formation of 9 is consistent with concomitant formations of SiR<sub>2</sub> units (2 and 10). The time course of the product yields monitored by <sup>1</sup>H NMR spectrum (see Figure S16 in the Supplementary Materials) indicated that 7 was initially formed and then 8 and 9 were generated in this reaction: after heating for 3 h, 7, 8, and 9 were observed in 26%, 3%, and 28% yields, respectively, while 19 h later, 7 disappeared and 8 and 9 were observed in 6% and 59% yields, respectively. Silicon clusters 7, 8, and 9 are moisture and air sensitive and isolated by careful recrystallization of the reaction mixture. Details of the structures of 7–9 will be discussed in the subsequent sections.



**Scheme 2.** Thermal transformation of 4. R = SiMe<sub>3</sub>.

Interestingly, thermal reaction of pure 7 at 60 °C in benzene-*d*<sub>6</sub> provided not only 8 and 9 but also 4. This result indicates that isomerization between 4 and 7 is reversible at 60 °C in solution, though we are not able to distinguish whether 8 and 9 were formed from 4 directly or via 7. While 8 remains intact after heating even at 80 °C for 10 h in benzene-*d*<sub>6</sub>, 9 was decomposed together with formation of 10 under the same conditions as monitored by <sup>1</sup>H NMR spectroscopy.

### 2.2. Molecular Structure of 7

XRD analysis exhibits that 7 has unsubstituted vertices at the Si3 and Si4 atoms that were shared by the bicyclo[1.1.0]tetrasilane moiety [Si1, Si2, Si3, and Si4] similar to 4 and the tricyclo[2.2.0.0<sup>2,5</sup>]hexasilane moiety [Si3, Si4, Si5, Si6, Si7, and Si8] (Figure 1). The Si3 and Si4 atoms adopt a highly distorted umbrella geometry which is very far from the typical tetrahedral configuration: the bond angles vary from 57.47(2)° [Si2–Si3–Si4] to 149.57(3)° [Si1–Si3–Si6] around the Si3 atom and from 56.02(2)° [Si2–Si4–Si3] to 140.10(3)° [Si2–Si4–Si5] around the Si4 atom. The distance between Si3

and Si4 [2.5477(8) Å] is longer than typical Si–Si single bond length [ca. 2.36 Å] [31] and those of the other Si–Si bonds in the silicon skeleton of **7** [2.3037(8)–2.4618(7) Å] but close to the distance between bridgehead unsubstituted silicon atoms in hexamesitylpentasila[1.1.1]propellane **11** [2.636(1) Å] [18] and siliconoids such as **12** [2.7076(8) Å] [13,14] (Figure 2).

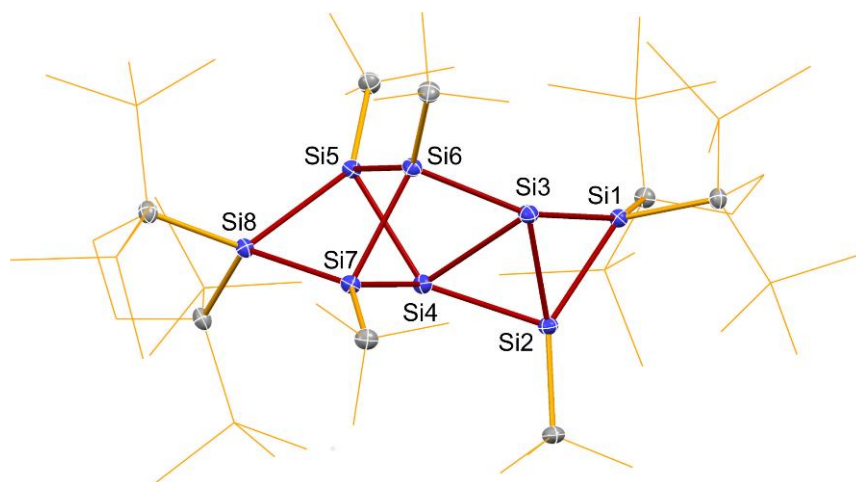


**Figure 1.** ORTEP drawing of **7** (atomic displacement parameters set at 50% probability; hydrogen atoms and thermal ellipsoids of selected carbon and silicon atoms omitted for clarity). Selected distances [Å] and angles [°]: Si1–Si2 2.3684(7), Si1–Si3 2.3798(8), Si2–Si3 2.3037(8), Si2–Si4 2.3422(8), Si3–Si4 2.5466(8), Si4–Si5 2.4005(8), Si4–Si7 2.4240(7), Si5–Si6 2.3563(8), Si5–Si8 2.4441(7), Si6–Si7 2.3440(8), Si7–Si8 2.4618(7), Si1–Si2–Si3–Si4 122.48(3).

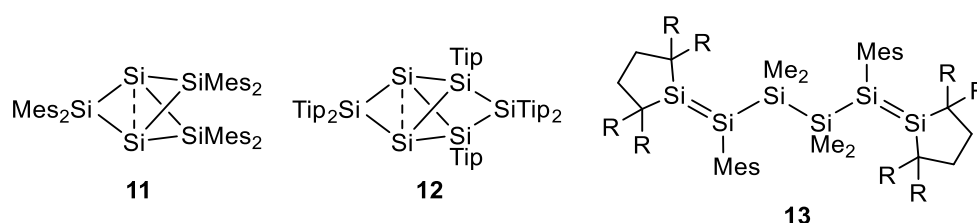


**Figure 2.** Related silicon clusters and a disilene. Mes = 2,4,6-trimethylphenyl, Tip = 2,4,6-triisopropylphenyl, R = SiMe<sub>3</sub>.

The <sup>1</sup>H NMR spectrum of **7** indicates a facile flipping of the bicyclo[1.1.0]tetrasilane moiety (Si1, Si2, Si3, and Si4) in solution on the NMR time scale: two *t*-Bu groups on Si5 and Si7 atoms were equally observed and four singlet signals for SiMe<sub>3</sub> groups on the terminal five-membered rings were observed with the same integral ratio. In the <sup>29</sup>Si NMR spectrum of **7**, a large distribution of chemical shifts [ $\delta$ Si = −191.9 (Si4), −66.3 (Si6), −20.0 (Si3), −12.0 (Si5, Si7), 7.5 (Si2), 42.2 (Si1), 64.7 (Si8) ppm] were observed similar to those observed for the reported siliconoids [13,14,18].

The UV–Vis spectrum of **7** in hexane exhibits several absorption bands tailed to ca. 600 nm with several shoulders as found in those of other molecular silicon clusters. The longest wavelength's absorption maximum was observed at 492 nm ( $\epsilon$  1400) (Figure 3). Judging from the results of the TD-DFT calculation of **7** at the B3LYP/6-311G(d)//B3PW91-D3/6-31G(d) level of theory (**7**<sub>opt</sub>), the band at 492 nm can be assigned to the transition from HOMO to LUMO. As shown in Figure 3b, HOMO and LUMO are mainly the  $\sigma$  and  $\sigma^*$  orbitals of the Si3–Si4 bond with the highly distorted geometry which is the longest Si–Si distance in the silicon framework as mentioned above.

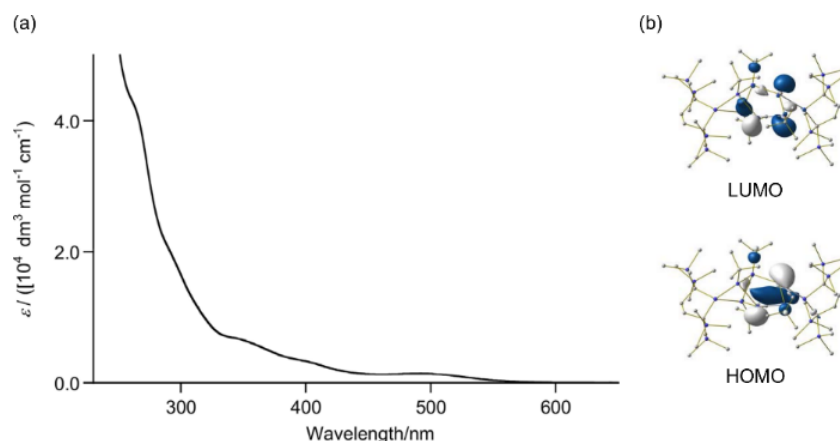


**Figure 3.** (a) UV-Vis spectrum of **7** in hexane at room temperature. (b) Frontier Kohn-Sham orbitals of **7** at the B3LYP-D3/6-311G(d)//B3PW91-D3/6-31G(d) level of theory (isosurface value =  $0.05 \text{ e}^- / \text{\AA}^3$ ).

### 2.3. Molecular Structure of **8**

Although purification of **8** was very difficult because of its very low yield, a few single crystals of **8** were luckily obtained after recrystallization from hexane. Accordingly, **8** was characterized by only XRD analysis and  $^1\text{H}$  NMR spectroscopy. XRD analysis exhibits that it has two silicon-silicon double bonds at both sides of a tricyclo[2.2.0.0<sup>2,5</sup>]hexasilane framework (Figure 4). The double-bond silicon atoms Si1, Si2, Si5, and Si6 lie on the crystallographic C2 axis. The Si1-Si2 [2.1570(12) Å] and Si5-Si6 [2.1641(12) Å] distances are within the range of the known silicon-silicon double bonds (2.118–2.289 Å) [32,33] and these Si=Si double-bond planes are almost perpendicular to each other with the dihedral angle between the least-square plane of the terminal silacyclopentane rings of 87.3°. The Si-Si single bond distances in the central tricyclo[2.2.0.0<sup>2,5</sup>]hexasilane skeleton [2.3496(8)–2.3641(9) Å] are similar to that of typical Si-Si single bonds (ca. 2.36 Å) [31] and reported tricyclo[2.2.0.0<sup>2,5</sup>]hexasilanes [2.33–2.47 Å] [13,34–36].

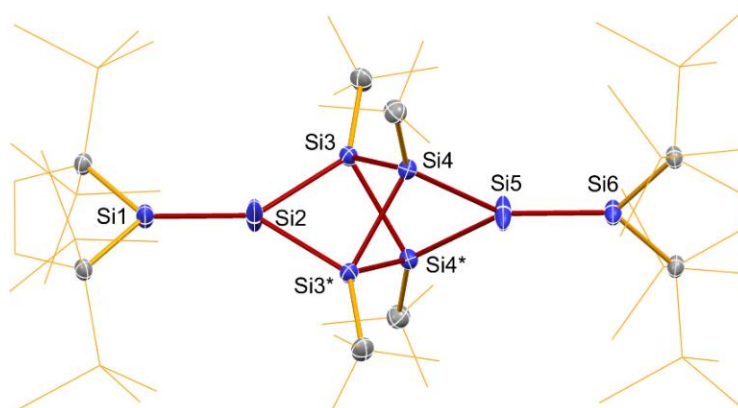


**Figure 4.** ORTEP drawing of **8** (atomic displacement parameters set at 50% probability; hydrogen atoms and thermal ellipsoids of selected carbon and silicon atoms omitted for clarity). Selected distances [Å] and angles [°]: Si1–Si2 2.1570(12), Si2–Si3 2.3570(9), Si3–Si4 2.3496(8), Si4–Si5 2.3641(9), Si5–Si6 2.1641(12), Si1–Si2–Si3 142.020(19), Si3–Si2–Si3\* 75.96(4), Si2–Si3–Si4 90.74(3), Si3–Si4–Si5 91.17(3), Si4–Si5–Si6 142.41(2), Si1–Si2–Si3–Si4 142.134(19), Si2–Si3–Si4–Si5 128.51(2).

In the UV-Vis spectrum of **8** in hexane, a distinct absorption band ( $\lambda_{\text{max}}$  451 nm) with a shoulder band (500 to 600 nm) was observed in the visible region (Figure 5a). This band is considerably redshifted compared to that observed for a structurally related bis(disilene) in which two Si=Si double bonds were connected by a Si-Si bond (**13**,  $\lambda_{\text{max}}$  = 403 nm, Figure 2). DFT calculation suggested that the

band in the visible region would be overlapped by a few bands due to  $\pi(\text{Si}=\text{Si})$  to  $\pi^*(\text{Si}=\text{Si})$  transitions. For compound **8** optimized at the B3PW91-D3/6-31G(d) level of theory ( $\mathbf{8}_{\text{opt}}$ ), HOMO ( $-4.47$  eV) and HOMO-1 ( $-4.50$  eV) are  $\pi(\text{Si}=\text{Si})$  orbitals, while LUMO ( $-1.47$  eV) and LUMO+1 ( $-1.17$  eV) are  $\pi^*(\text{Si}=\text{Si})$  orbitals (Figure 5b). While HOMO and HOMO-1 are almost degenerated, the difference in energy between LUMO and LUMO+1 was relatively large (0.30 eV). This large energy difference would result from considerable interaction between two  $\pi^*(\text{Si}=\text{Si})$  orbitals through the central silicon cage. TD-DFT calculation of  $\mathbf{8}_{\text{opt}}$  at the B3LYP/6-311G(d) [hexane]//B3PW91-D3/6-31G(d) level of theory predicts that the major peak observed at 451 nm involves a combination of HOMO-1 to LUMO+1 and HOMO to LUMO+1 transitions, while the shoulder band involves HOMO to LUMO and HOMO-1 to LUMO transitions. The spectral feature of **8** is consistent with the substantial interactions between two Si=Si double bonds through the central silicon cages.

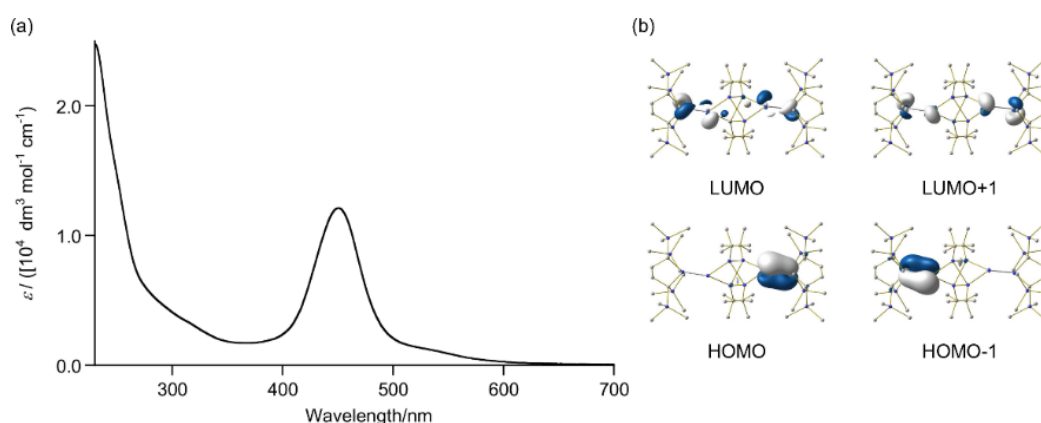


**Figure 5.** (a) UV-Vis spectrum of **8** in hexane at room temperature. (b) Frontier Kohn-Sham orbitals of **8** at the B3LYP-D3/6-311G(d)//B3PW91-D3/6-31G(d) level of theory (isosurface value =  $0.05 \text{ e}^- / \text{\AA}^3$ ).

#### 2.4. Molecular Structure of **9**

The XRD analysis indicates that **9** is also a silicon cluster classified as a siliconoid having unsubstituted vertices at Si2 and Si3 atoms with a hexasila[2.1.1]propellane skeleton in which two wings (Si4 and Si5–Si6) are bridged by Si7 atom (Figure 6). To the best of our knowledge, this is the first example of a silicon cluster having [2.1.1]propellane skeleton, although persilapropellane family including hexamesitylpentasila[1.1.1]propellane **11** (Figure 2) [18] and its bridged siliconoids [13,14] have been synthesized as isolable molecules. Cluster **9** can also be seen as a hexasilaprismane (Si2–Si7) in which two skeletal silicon atoms (Si2 and Si3) are bridged by one silicon atom (Si1). The Si2 and Si3 atoms adopt an umbrella-type inverted tetrahedral geometry as observed for bridgehead silicon atoms of pentasila[1.1.1]properanes [13,14,18]. The Si2–Si3 distance [2.6829(8) Å] is comparable with the distances between silicon atom with an umbrella geometry in hexamesitylpentasila[1.1.1]propellane **11** [2.636(1) Å] [18] and siliconoids such as **12** [2.7076(8) Å] (Figure 2) [13,14].

The  $^{29}\text{Si}$  NMR spectrum of **9** showed five signals due to skeletal silicon nuclei at  $-159.5$  (Si2, Si3),  $-60.3$  (Si7),  $2.3$  (Si5, Si6),  $26.5$  (Si1),  $123.3$  (Si4) ppm, which were assigned on the basis of a  $^1\text{H}$ - $^{29}\text{Si}$  HMBBC spectrum. The highfield-shifted  $^{29}\text{Si}$  NMR resonance due to the unsubstituted vertices of **9** ( $\delta\text{Si} = -159.5$ ) is similar to those of pentasila[1.1.1]propellane **11** [ $\delta\text{Si} = -273.2$  [18]] and its bridged siliconoid **12** [ $\delta\text{Si} = -274.2$  [13]], while the considerably downfieldshift of Si4 nuclei in **9** resembles that of **12** [ $\delta\text{Si} = 174.6$ ] [13]. The geometry around the hexasilaprismane framework in **9** except for the Si2 and Si3 atoms resembles to those of the reported hexasilaprismanes [10,36,37].

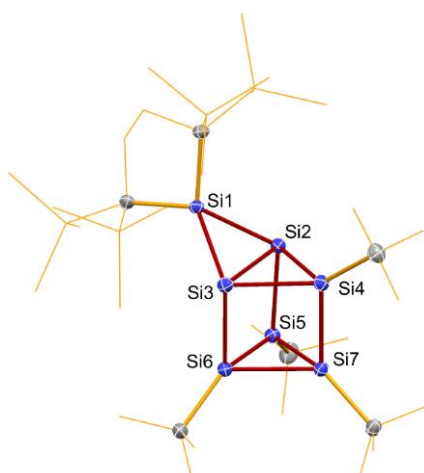


**Figure 6.** ORTEP drawing of **9** (atomic displacement parameters set at 50% probability; hydrogen atoms and thermal ellipsoids of selected carbon and silicon atoms omitted for clarity). Selected distances [Å] and angles [°]: Si1–Si2 2.3813(8), Si2–Si3 2.6829(8), Si2–Si4 2.3645(8), Si2–Si5 2.3738(8), Si3–Si4 2.3566(8), Si3–Si6 2.3804(8), Si4–Si7 2.3051(8), Si5–Si6 2.3292(8), Si5–Si7 2.3435(9), Si6–Si7 2.3511(8), Si2–Si1–Si3 68.86(3), Si1–Si2–Si3 55.26(2), Si1–Si2–Si4 102.08(3), Si1–Si2–Si5 117.64(3), Si4–Si2–Si5 88.85(3), Si1–Si3–Si2 55.88(2), Si1–Si3–Si4 102.85(3), Si1–Si3–Si6 115.41(3), Si4–Si3–Si6 88.32(3), Si1–Si2–Si3–Si4 142.33(4).

In the UV–Vis spectrum in hexane, **9** exhibits a distinct absorption band at 511 nm ( $\epsilon$  2700) (Figure 7), which is similar to the absorption bands observed for siliconoids **11** and **12** (Figure 2) but in contrast to those for hexasilaprismanes showing normally only weak absorption tailing to 500 nm [10,36,37]. TD-DFT calculation of **9** predicted that this band should be assigned to HOMO  $\rightarrow$  LUMO and HOMO–1  $\rightarrow$  LUMO transitions. HOMO–1 and LUMO involve mainly  $\sigma$  and  $\sigma^*$  orbitals of the interbridgehead Si2–Si3 bond with the umbrella geometry, while HOMO is  $\sigma$  orbitals of the Si–Si bond in the silicon framework. The characteristic absorption band observed in **9** would result from the presence of the unsubstituted silicon vertices with an inverted geometry.

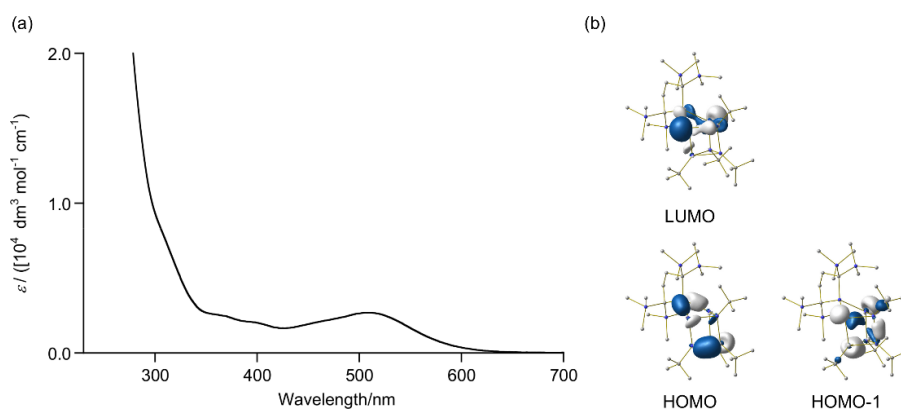


**Figure 7.** (a) UV–Vis spectrum of **9** in hexane at room temperature. (b) Frontier Kohn–Sham orbitals of **9** at the B3LYP-D3/6-311G(d)//B3PW91-D3/6-31G(d) level of theory (isosurface value =  $0.05 \text{ e}^- / \text{Å}^3$ ).

## 2.5. Theoretical Study

Although the detailed mechanism for transformation from **4** to **7–9** remains unclear at this moment, it should be worthy to discuss the relative stability of  $\text{Si}_8\text{R}_8$  isomers **4**, **6**, **7**, **8**. In Table 1, relative energies of the clusters calculated at the B3PW91-D3/6-31G(d) level are shown and all optimized structures (**4**<sub>opt</sub>, **6**<sub>opt</sub>, **7**<sub>opt</sub>, **8**<sub>opt</sub>, and **9**<sub>opt</sub>) were in agreement with the experimentally observed structures. Formations of **6**<sub>opt</sub> and **7**<sub>opt</sub> from **4**<sub>opt</sub> are predicted to be very slightly endoergonic, while generation of **8**<sub>opt</sub>

and  $9_{\text{opt}}+2_{\text{opt}}$  and from  $4_{\text{opt}}$  are exoergonic at 348.14 K, which is consistent with the experimental results. In contrast to the predicted high thermal stability of  $8_{\text{opt}}$ , the yield of **8** was considerably low. As silylene **2** decomposes quickly to **10** at 348 K [38], formation of **9** is expected to be irreversible under the thermal conditions. The irreversible formation of **9** and the higher activation barrier for formation of **8** compared to those for other reactions may be responsible for the low yield of **8**. Although the reason for the higher stability of  $8_{\text{opt}}$  compared to other isomers remains unclear, the absence of the highly strained structure such as bicyclo[1.1.0]tetrasilane moiety and the umbrella geometry as found in  $4_{\text{opt}}$ ,  $6_{\text{opt}}$ , and  $7_{\text{opt}}$  may be mainly responsible for the relative stability of  $8_{\text{opt}}$ .

**Table 1.** Relative free energies for  $\text{Si}_8\text{R}_8$  isomers calculated at the B3PW91-D3/6-31G(d) level of theory.

Compound	$\Delta G(298.15 \text{ K})$ [kJ/mol]	$\Delta G(348.15 \text{ K})$ [kJ/mol]
$4_{\text{opt}}$	0.0	0.0
$6_{\text{opt}}$	+16.2	+14.6
$7_{\text{opt}}$	+14.2	+14.6
$8_{\text{opt}}$	−71.8	−77.5
$9_{\text{opt}} + 2_{\text{opt}}$	+14.9	−0.1

It is also noteworthy to compare with other possible  $\text{Si}_8\text{R}_8$  isomers. Theoretical study of  $\text{Si}_8\text{H}_8$  species demonstrated that a silicon cluster bearing a bicyclo[1.1.0]butane moiety with  $C_2$  symmetry ( $14^{\text{H}}$  in Figure 8) has been located theoretically as the most stable isomer which is 30.9 kJ/mol lower in energy than the second stable octasilacubane  $15^{\text{H}}$  at the B3LYP/6-31G(d) level of theory [39]. While isolable  $\text{Si}_8\text{R}_8$  species such as octasilacubane **15** [40–45] and octasilacuneane **16** [19] have been reported, the  $\text{Si}_8\text{R}_8$  clusters in our study such as **4**, **6**, **7**, and **8** do not provide such stable isomers. Two silicon vertices of the  $\text{Si}_8\text{R}_8$  clusters in this study have two alkyl groups, while two silicon vertices are unsubstituted, which would lead to a unique transformation reaction without involving the stable isomers such as octacubane.

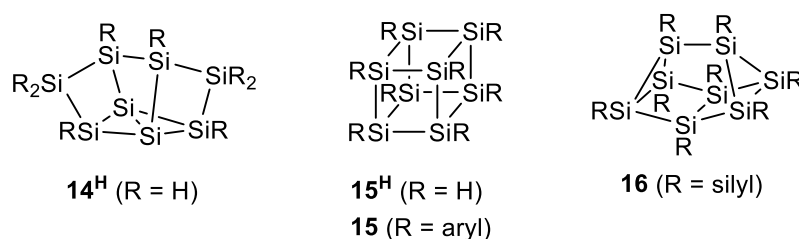


**Figure 8.** Examples of related  $\text{Si}_8\text{R}_8$  isomers.

### 3. Materials and Methods

#### 3.1. General Procedures

All reactions treating air-sensitive compounds were carried out under nitrogen atmosphere using a high-vacuum line and standard Schlenk techniques, or a glove box, as well as dry and oxygen-free solvents. NMR spectra were recorded on a Bruker Avance 500 FT NMR spectrometer (Bruker Japan, Yokohama, Japan). The  $^1\text{H}$  and  $^{13}\text{C}$  NMR chemical shifts were referenced to residual  $^1\text{H}$  and  $^{13}\text{C}$  signals of the solvents, benzene- $d_6$  ( $^1\text{H}$   $\delta$  7.16;  $^{13}\text{C}$   $\delta$  128.0). The  $^{29}\text{Si}$  NMR chemical shifts were relative to  $\text{Me}_4\text{Si}$  in ppm ( $\delta$  0.00). Sampling of air-sensitive compounds was carried out using a VAC NEXUS 100027 type glove box (Vacuum Atmospheres Co., Hawthorne, CA, USA). Reactions at low temperatures were performed by using an EYELA PSL-1400 cryobath (Tokyo Rikakikai Co, Ltd, Tokyo, Japan). UV–Vis spectra were recorded on a JASCO V-660 spectrometer (JASCO, Tokyo, Japan).

### 3.2. Materials

Benzene, benzene-*d*<sub>6</sub>, diethyl ether, hexane, tetrahydrofuran (THF), and toluene were dried over LiAlH<sub>4</sub>, and then distilled prior to use by using the vacuum line. Compound **4** was prepared according to the procedure reported in the literature [22].

### 3.3. Thermolysis of **4**

In a J. Young NMR tube, **4** (5.0 mg, 0.0044 mmol) was dissolved in benzene-*d*<sub>6</sub> (0.5 mL). The mixture was heated for 22 h at 75 °C, monitored by <sup>1</sup>H NMR spectroscopy (Figure S16). After heating the mixture for 3 h, compounds **7** (26%), **8** (3%), and **9** (28%) were formed (Figure S1). After heating for a total of 22 h, only **8** (6%) and **9** (59%) were observed (Figure S2). The yields of **7–9** were determined by <sup>1</sup>H NMR spectroscopy using ferrocene as an internal standard.

### 3.4. Isolation of **7**

In a Schlenk tube (30 mL) equipped with a magnetic stir bar, compound **4** (150 mg, 0.131 mmol) and benzene (15 mL) were placed. The reaction mixture was heated at 75 °C for 3 h. Benzene was removed in vacuo. Recrystallization from hexane at –35 °C gave **4**. Recrystallization of the mother liquor from toluene at –35 °C gave cluster **7** as reddish orange crystals (11.4 mg, 0.0100 mmol) in 8.0% yield.

**7**: reddish orange crystals; mp. 138 °C (decomp.); <sup>1</sup>H NMR (C<sub>6</sub>D<sub>6</sub>, 500 MHz, 298 K) δ 0.40 (s, 18H, SiMe<sub>3</sub>), 0.45 (s, 18H, SiMe<sub>3</sub>), 0.46 (s, 18H, SiMe<sub>3</sub>), 0.52 (s, 18H, SiMe<sub>3</sub>), 1.52 (s, 18H, *t*-Bu), 1.53 (s, 9H, *t*-Bu), 1.57 (s, 9H, *t*-Bu), 1.94–2.00 (m, 4H, CH<sub>2</sub>), 2.03 (s, 4H, CH<sub>2</sub>); <sup>13</sup>C NMR (C<sub>6</sub>D<sub>6</sub>, 125 MHz, 298 K) δ 4.8 (SiMe<sub>3</sub>), 5.8 (SiMe<sub>3</sub>), 6.2 (SiMe<sub>3</sub>), 6.6 (SiMe<sub>3</sub>), 17.5 (C), 19.5 (C), 20.6 (C), 26.8 (C), 32.0 (C(CH<sub>3</sub>)<sub>3</sub>), 32.3 (C), 33.4 (C(CH<sub>3</sub>)<sub>3</sub>), 34.2 (C), 35.1 (CH<sub>2</sub>), 35.6 (CH<sub>2</sub>), 35.9 (C(CH<sub>3</sub>)<sub>3</sub>), 36.3 (CH<sub>2</sub>); <sup>29</sup>Si NMR (C<sub>6</sub>D<sub>6</sub>, 99 MHz, 298 K) δ –191.9 (Si4), –66.3 (Si8), –20.0 (Si2), –12.0 (Si5, Si7), 2.60 (SiMe<sub>3</sub>), 3.01 (SiMe<sub>3</sub>), 3.66 (2 × SiMe<sub>3</sub>), 7.53 (Si3), 42.2 (Si1), 64.7 (Si6); UV/vis (in hexane): λ<sub>max</sub>/nm (ε) 492 (1400), 405 (sh, 3100), 351 (sh, 6500); HRMS (APCI) *m/z* ([M]<sup>+</sup> was not observed but [M + H + O<sub>2</sub>]<sup>+</sup> was found probably because **7** is so reactive that it was partially oxidized and/or hydrolyzed before injecting the sample into the instrument) calcd for C<sub>48</sub>H<sub>117</sub>O<sub>2</sub>Si<sub>16</sub>: 1173.5356; found: 1173.5353; anal. calcd for C<sub>48</sub>H<sub>116</sub>Si<sub>16</sub>: C, 50.45; H, 10.23; found: C, 50.83; H, 9.90.

### 3.5. Isolation of **8** and **9**

In a Schlenk tube (30 mL) equipped with a magnetic stir bar, compound **4** (104.0 mg, 0.0910 mmol) and benzene (15 mL) were placed. The reaction mixture was heated at 75 °C for 20 h. The volatiles were removed in vacuo. Recrystallization from hexane at –35 °C gave **8** as an orange powder (2.6 mg, 0.0023 mmol) in 3% yield. Recrystallization of the mother liquor from diethyl ether at –35 °C gave **9** as red crystals (20.4 mg, 0.026 mmol) in 29% yield.

**8**: orange crystals; <sup>1</sup>H NMR (C<sub>6</sub>D<sub>6</sub>, 500 MHz, 299 K) δ 0.39 (s, 72H, SiMe<sub>3</sub>), 1.71 (s, 36H, *t*-Bu), 1.98 (s, 8H, CH<sub>2</sub>); UV/vis (in hexane): λ<sub>max</sub>/nm (ε) 540 (sh, 1100), 451 (12000).

**9**: red crystals; mp. 164 °C (decomp); <sup>1</sup>H NMR (C<sub>6</sub>D<sub>6</sub>, 500 MHz, 299 K) δ 0.31 (s, 18H, SiMe<sub>3</sub>), 0.54 (s, 18H, SiMe<sub>3</sub>), 1.30 (s, 18H, *t*-Bu), 1.35 (s, 9H, *t*-Bu), 1.39 (s, 9H, *t*-Bu), 1.90–2.06 (m, 8H, CH<sub>2</sub>); <sup>13</sup>C NMR (C<sub>6</sub>D<sub>6</sub>, 125 MHz, 300 K) δ 5.1 (SiMe<sub>3</sub>), 5.6 (SiMe<sub>3</sub>), 15.5 (C), 17.7 (C), 24.9 (C), 25.8 (C), 30.4 (C), 31.3 (C(CH<sub>3</sub>)<sub>3</sub>), 31.5 (C(CH<sub>3</sub>)<sub>3</sub>), 32.0 (C(CH<sub>3</sub>)<sub>3</sub>), 35.5 (CH<sub>2</sub>), 36.9 (CH<sub>2</sub>); <sup>29</sup>Si NMR (C<sub>6</sub>D<sub>6</sub>, 99 MHz, 299 K) δ –159.5 (Si2, Si3), –60.3 (Si7), 2.3 (Si5, Si6), 3.6 (SiMe<sub>3</sub>), 5.3 (SiMe<sub>3</sub>), 26.5 (Si1), 123.3 (Si4); UV/vis (in hexane): λ<sub>max</sub>/nm (ε) 511 (2700), 260 (28000); HRMS (APCI) *m/z* ([M]<sup>+</sup> was missing but [M + H<sub>3</sub> + O<sub>4</sub>]<sup>+</sup> was found probably because **9** is highly reactive and it was partially oxidized and/or hydrolyzed before injecting the sample into the instrument) calcd for C<sub>32</sub>H<sub>79</sub>O<sub>4</sub>Si<sub>11</sub>: 835.3435; found: 835.3437; anal. calcd for C<sub>32</sub>H<sub>76</sub>Si<sub>11</sub>: C, 49.92; H, 9.95; found: C, 49.90; H, 9.81.

### 3.6. X-ray Analysis

Recrystallization from toluene (7), hexane (8), and diethyl ether (9) at  $-35\text{ }^{\circ}\text{C}$  gave single crystals suitable for data collection. The single crystals coated by Apiezon<sup>®</sup> grease were mounted on the glass fiber and transferred to the cold gas stream of the diffractometer. X-ray data were collected on a BrukerAXS APEXII diffractometer (Bruker Japan, Yokohama, Japan) with graphite monochromated Mo K $\alpha$  radiation ( $\lambda = 0.71073\text{ \AA}$ ). The data were corrected for Lorentz and polarization effects. An empirical absorption correction based on the multiple measurement of equivalent reflections was applied using the program SADABS [46]. The structures were solved by direct methods and refined by full-matrix least squares against  $F^2$  using all data (SHELXL-2014/7) [47]. CCDC-1863288–1863290 contain the supplementary crystallographic data for this paper. These data can be obtained free of charge via <http://www.ccdc.cam.ac.uk/conts/retrieving.html> (or from the CCDC, 12 Union Road, Cambridge CB2 1EZ, UK; Fax: +44 1223 336033; E-mail: deposit@ccdc.cam.ac.uk).

7: CCDC-1863288; [code si302a]; 100 K;  $\text{C}_{48}\text{H}_{116}\text{Si}_{16}\cdot(\text{C}_7\text{H}_8)_{2.5}$ ; Fw 1373.17; triclinic; space group  $P-1$  (#2),  $a = 11.5327(18)\text{ \AA}$ ,  $b = 17.883(3)\text{ \AA}$ ,  $c = 21.560(3)\text{ \AA}$ ,  $\alpha = 69.416(2)^{\circ}$ ,  $\beta = 85.458(2)^{\circ}$ ,  $\gamma = 76.379(2)^{\circ}$ ,  $V = 4045.5(11)\text{ \AA}^3$ ,  $Z = 2$ ,  $D_{\text{calcd}} = 1.127\text{ mg/m}^3$ ,  $R1 = 0.0357$  ( $I > 2\sigma(I)$ ),  $wR2 = 0.0941$  (all data), GOF = 1.062.

8: CCDC-1863289; [code si303a]; 100 K;  $\text{C}_{48}\text{H}_{116}\text{Si}_{16}$ ; Fw 1142.84; monoclinic; space group  $C2/c$  (#15),  $a = 21.538(2)\text{ \AA}$ ,  $b = 17.9167(19)\text{ \AA}$ ,  $c = 20.792(3)\text{ \AA}$ ,  $\beta = 118.8750(10)^{\circ}$ ,  $V = 7026.1(15)\text{ \AA}^3$ ,  $Z = 4$ ,  $D_{\text{calcd}} = 1.080\text{ mg/m}^3$ ,  $R1 = 0.0363$  ( $I > 2\sigma(I)$ ),  $wR2 = 0.0910$  (all data), GOF = 1.077.

9: CCDC-1863290; [code si301a]; 100 K;  $\text{C}_{32}\text{H}_{76}\text{Si}_{11}$ ; Fw 769.92; orthorhombic; space group  $Pbca$  (#61),  $a = 11.3287(13)\text{ \AA}$ ,  $b = 17.976(2)\text{ \AA}$ ,  $c = 46.325(5)\text{ \AA}$ ,  $V = 9433.6(19)\text{ \AA}^3$ ,  $Z = 8$ ,  $D_{\text{calcd}} = 1.084\text{ mg/m}^3$ ,  $R1 = 0.0377$  ( $I > 2\sigma(I)$ ),  $wR2 = 0.0839$  (all data), GOF = 1.111.

### 3.7. Theoretical Study

All theoretical calculations were performed using a Gaussian 09 [48] and GRRM14 programs [49,50]. Geometry optimization of 2, 4, 6, 7, 8, and 9 ( $2_{\text{opt}}$ ,  $4_{\text{opt}}$ ,  $6_{\text{opt}}$ ,  $7_{\text{opt}}$ ,  $8_{\text{opt}}$ , and  $9_{\text{opt}}$ ) were carried out at the B3PW91-D3/6-31G(d) level of theory. The atomic coordinates of all optimized structures were summarized in a .xyz file (optimized structures.xyz).

## 4. Conclusions

$\text{Si}_3\text{R}_8$  cluster 4 transforms into novel silicon clusters 7, 8, and 9, bearing unprecedented silicon frameworks accompanied by elimination of the  $\text{R}_2\text{Si}$  (silylene) unit under a mild thermal condition. Reversible isomerization between 4 and 7 was observed. XRD analyses exhibit that both 7 and 9 have two unsubstituted skeletal silicon atoms classified as siliconoids, while 8 has two Si=Si double bonds. A large dispersion of  $^{29}\text{Si}$  chemical shifts was observed for 7 and 9 as found in the reported siliconoids. The observed transformation of molecular silicon clusters involving substantially different molecular structures and electronic properties suggests that unsaturated molecular silicon clusters have a great potential to provide various molecular silicon clusters bearing unprecedented structures and properties.

**Supplementary Materials:** The following are available online at <http://www.mdpi.com/2304-6740/6/4/107/s1>, Figures S1–S15: NMR spectra of 7–9, Figure S16: Time course of the product yields during thermolysis of 7, Figures S17–S19: UV–Vis spectra of 7–9, Tables S1–S5: Transition Energy, Wavelength, and Oscillator Strengths of the Electronic Transition of  $4_{\text{opt}}$ ,  $6_{\text{opt}}$ – $9_{\text{opt}}$ , a xyz file (“optimized structures.xyz”): the atomic coordinates and energies of  $4_{\text{opt}}$ ,  $6_{\text{opt}}$ – $9_{\text{opt}}$ . Cif and checkCif files.

**Author Contributions:** Investigation, N.A. and S.I.; Project administration, T.I.; Writing—original draft, N.A.; Writing—review & editing, N.A., S.I., and T.I.

**Funding:** This work was supported by JSPS KAKENHI grant JP25248010, JP17H03015 (Takeaki Iwamoto), and Grant-in-Aid for JSPS Fellows (Naohiko Akasaka).

**Conflicts of Interest:** The authors declare no conflict of interest.

## References

1. Hengge, E.; Janoschek, R. Homocyclic silanes. *Chem. Rev.* **1995**, *95*, 1495–1526. [[CrossRef](#)]
2. Sekiguchi, A.; Sakurai, H. Cage and cluster compounds of silicon, germanium, and tin. *Adv. Organomet. Chem.* **1995**, *37*, 1–38. [[CrossRef](#)]
3. Sekiguchi, A.; Nagase, S. Polyhedral silicon compounds. In *The Chemistry of Organic Silicon Compounds*; Rappoport, Z., Apeloig, Y., Eds.; Wiley: Chichester, UK, 1998; Volume 2, pp. 119–152.
4. Hengge, E.; Stüger, H. Recent advances in the chemistry of cyclopolysilanes. In *The Chemistry of Organic Silicon Compounds*; Rappoport, Z., Apeloig, Y., Eds.; Wiley: Chichester, UK, 1998; Volume 2, pp. 2177–2216.
5. Marschner, C. Oligosilanes. In *Structure and Bonding 156, Functional Molecular Silicon Compounds I. Regular Oxidation States*; Scheschkewitz, D., Ed.; Springer: New York, NY, USA, 2014; Volume 156, pp. 163–228.
6. Lyon, J.T.; Gruene, P.; Fielicke, A.; Meijer, G.; Janssens, E.; Claes, P.; Lievens, P. Structures of silicon cluster cations in the gas phase. *J. Am. Chem. Soc.* **2009**, *131*, 1115–1121. [[CrossRef](#)] [[PubMed](#)]
7. Peppernick, S.J.; Gunaratne, K.D.D.; Castleman, A.W. The relative abundances of silicon hydride clusters,  $\text{Si}_n\text{H}_x^-$  ( $n = 8\text{--}12$  and  $0 \leq x \leq 25$ ), investigated with high-resolution time-of-flight mass spectrometry. *Int. J. Mass. Spectr.* **2010**, *290*, 65–71. [[CrossRef](#)]
8. Haertelt, M.; Lyon, J.T.; Claes, P.; de Haeck, J.; Lievens, P.; Fielicke, A. Gas-phase structures of neutral silicon clusters. *J. Chem. Phys.* **2012**, *136*, 064301. [[CrossRef](#)] [[PubMed](#)]
9. Berger, R.J.; Rzepa, H.S.; Scheschkewitz, D. Ring currents in the dismutational aromatic  $\text{Si}_6\text{R}_6$ . *Angew. Chem. Int. Ed.* **2010**, *49*, 10006–10009. [[CrossRef](#)] [[PubMed](#)]
10. Abersfelder, K.; Russell, A.; Rzepa, H.S.; White, A.J.P.; Haycock, P.R.; Scheschkewitz, D. Contraction and expansion of the silicon scaffold of stable  $\text{Si}_6\text{R}_6$  isomers. *J. Am. Chem. Soc.* **2012**, *134*, 16008–16016. [[CrossRef](#)] [[PubMed](#)]
11. Scheschkewitz, D. A molecular silicon cluster with a “naked” vertex atom. *Angew. Chem. Int. Ed.* **2005**, *44*, 2954–2956. [[CrossRef](#)] [[PubMed](#)]
12. Abersfelder, K.; White, A.J.P.; Rzepa, H.S.; Scheschkewitz, D. A tricyclic aromatic isomer of hexasilabenzene. *Science* **2010**, *327*, 564–566. [[CrossRef](#)] [[PubMed](#)]
13. Abersfelder, K.; White, A.J.P.; Berger, R.J.F.; Rzepa, H.S.; Scheschkewitz, D. A stable derivative of the global minimum on the  $\text{Si}_6\text{H}_6$  potential energy surface. *Angew. Chem., Int. Ed.* **2011**, *50*, 7936–7939. [[CrossRef](#)] [[PubMed](#)]
14. Willmes, P.; Leszczynska, K.; Heider, Y.; Abersfelder, K.; Zimmer, M.; Huch, V.; Scheschkewitz, D. Isolation and versatile derivatization of an unsaturated anionic silicon cluster (siliconoid). *Angew. Chem. Int. Ed.* **2016**, *55*, 2907–2910. [[CrossRef](#)] [[PubMed](#)]
15. Fischer, G.; Huch, V.; Mayer, P.; Vasisht, S.K.; Veith, M.; Wiberg, N.  $\text{Si}_8(\text{Si}t\text{Bu}_3)_6$ : A hitherto unknown cluster structure in silicon chemistry. *Angew. Chem. Int. Ed.* **2005**, *44*, 7884–7887. [[CrossRef](#)] [[PubMed](#)]
16. Klapötke, T.M.; Vasisht, S.K.; Fischer, G.; Mayer, P. A reactive  $\text{Si}_4$  cage:  $\text{K}(\text{Si}t\text{Bu}_3)_3\text{Si}_4$ . *J. Organomet. Chem.* **2010**, *695*, 667–672. [[CrossRef](#)]
17. Klapötke, T.M.; Vasisht, S.K.; Mayer, P. Spirocycle  $(\text{Si}t\text{Bu}_3)_6\text{Si}_9\text{Cl}_2$ : The first of its kind among group 14 elements. *Eur. J. Inorg. Chem.* **2010**, *2010*, 3256–3260. [[CrossRef](#)]
18. Nied, D.; Koppe, R.; Kloppe, W.; Schnockel, H.; Breher, F. Synthesis of a pentasilapropellane. Exploring the nature of a stretched silicon–silicon bond in a nonclassical molecule. *J. Am. Chem. Soc.* **2010**, *132*, 10264–10265. [[CrossRef](#)] [[PubMed](#)]
19. Ishida, S.; Otsuka, K.; Toma, Y.; Kyushin, S. An organosilicon cluster with an octasilacuneane core: A missing silicon cage motif. *Angew. Chem. Int. Ed.* **2013**, *52*, 2507–2510. [[CrossRef](#)] [[PubMed](#)]
20. Tsurusaki, A.; Iizuka, C.; Otsuka, K.; Kyushin, S. Cyclopentasilane-fused hexasilabenzvalene. *J. Am. Chem. Soc.* **2013**, *135*, 16340–16343. [[CrossRef](#)] [[PubMed](#)]
21. Tsurusaki, A.; Kamiyama, J.; Kyushin, S. Tetrasilane-bridged bicyclo[4.1.0]heptasil-1-ene. *J. Am. Chem. Soc.* **2014**, *136*, 12896–12898. [[CrossRef](#)] [[PubMed](#)]
22. Iwamoto, T.; Akasaka, N.; Ishida, S. A heavy analogue of the smallest bridgehead alkene stabilized by a base. *Nat. Commun.* **2014**, *5*, 5353. [[CrossRef](#)] [[PubMed](#)]
23. Hamers, R.J.; Köhler, U.K.; Demuth, J.E. Nucleation and growth of epitaxial silicon on Si(001) and Si(111) surfaces by scanning tunneling microscopy. *Ultramicroscopy* **1989**, *31*, 10–19. [[CrossRef](#)]

24. Swihart, M.T.; Girshick, S.L. Thermochemistry and kinetics of silicon hydride cluster formation during thermal decomposition of silane. *J. Phys. Chem. B* **1999**, *103*, 64–76. [[CrossRef](#)]
25. Swihart, M.T.; Girshick, S.L. Ab initio structures and energetics of selected hydrogenated silicon clusters containing six to ten silicon atoms. *Chem. Phys. Lett.* **1999**, *307*, 527–532. [[CrossRef](#)]
26. Li, C.P.; Li, X.J.; Yang, J.C. Silicon hydride clusters  $\text{Si}_5\text{H}_n$  ( $n = 3\text{--}12$ ) and their anions: Structures, thermochemistry, and electron affinities. *J. Phys. Chem. A* **2006**, *110*, 12026–12034. [[CrossRef](#)] [[PubMed](#)]
27. Singh, R. Effect of hydrogen on ground state properties of silicon clusters ( $\text{Si}_n\text{H}_m$ ;  $n = 11\text{--}15$ ,  $m = 0\text{--}4$ ): A density functional based tight binding study. *J. Phys. Condens. Matt.* **2008**, *20*, 045226. [[CrossRef](#)]
28. Adamczyk, A.J.; Broadbelt, L.J. Thermochemical property estimation of hydrogenated silicon clusters. *J. Phys. Chem. A* **2011**, *115*, 8969–8982. [[CrossRef](#)] [[PubMed](#)]
29. Gapurenko, O.A.; Minyaev, R.M.; Minkin, V.I. Silicon analogues of pyramidane: A quantum-chemical study. *Mendeleev Commun.* **2012**, *22*, 8–10. [[CrossRef](#)]
30. Thingna, J.; Prasad, R.; Auluck, S. Photo-absorption spectra of small hydrogenated silicon clusters using the time-dependent density functional theory. *J. Phys. Chem. Solids* **2011**, *72*, 1096–1100. [[CrossRef](#)]
31. Kaftory, M.; Kapon, M.; Botoshansky, M. The structural chemistry of organosilicon compounds. In *The Chemistry of Organic Silicon Compounds*; Rappoport, Z., Apeloig, Y., Eds.; Wiley: Chichester, UK, 1998; Volume 2, pp. 181–266.
32. Okazaki, R.; West, R. Chemistry of stable disilenes. *Adv. Organomet. Chem.* **1996**, *39*, 231–273. [[CrossRef](#)]
33. Kira, M.; Iwamoto, T. Progress in the chemistry of stable disilenes. *Adv. Organomet. Chem.* **2006**, *54*, 73–148. [[CrossRef](#)]
34. Kabe, Y.; Kuroda, M.; Honda, Y.; Yamashita, O.; Kawase, T.; Masamune, S. Reductive oligomerization of 1,2-di-*tert*-butyl-1,1,2,2-tetrachlorodisilane: The tricyclo[2.2.0.0<sup>2,5</sup>]hexasilane and tetracyclo[3.3.0.0<sup>2,7</sup>.0<sup>3,6</sup>]octasilane systems. *Angew. Chem. Int. Ed. Engl.* **1988**, *27*, 1725–1727. [[CrossRef](#)]
35. Iwamoto, T.; Uchiyama, K.; Kabuto, C.; Kira, M. Synthesis of tricyclo[3.1.0.0<sup>2,4</sup>]hexasilane and its photochemical isomerization to tricyclo[2.2.0.0<sup>2,5</sup>]hexasilane. *Chem. Lett.* **2007**, *36*, 368–369. [[CrossRef](#)]
36. Li, Y.; Li, J.; Zhang, J.; Song, H.; Cui, C. Isolation of  $\text{R}_6\text{Si}_6$  dianion: A bridged tricyclic isomer of dianionic hexasilabenzene. *J. Am. Chem. Soc.* **2018**, *140*, 1219–1222. [[CrossRef](#)] [[PubMed](#)]
37. Sekiguchi, A.; Yatabe, T.; Kabuto, C.; Sakurai, H. The missing hexasilaprismane: Synthesis, x-ray analysis and photochemical reactions. *J. Am. Chem. Soc.* **1993**, *115*, 5853–5854. [[CrossRef](#)]
38. Kira, M.; Ishida, S.; Iwamoto, T.; Kabuto, C. The first isolable dialkylsilylene. *J. Am. Chem. Soc.* **1999**, *121*, 9722–9723. [[CrossRef](#)]
39. Tang, M.; Lu, W.; Wang, C.Z.; Ho, K.M. Search for most stable structure of  $\text{Si}_8\text{H}_8$  cluster. *Chem. Phys. Lett.* **2003**, *377*, 413–418. [[CrossRef](#)]
40. Matsumoto, H.; Higuchi, K.; Hoshino, Y.; Koike, H.; Naoi, Y.; Nagai, Y. The first octasilacubane system: Synthesis of octakis-(*t*-butyldimethylsilyl)pentacyclo[4.2.0.0<sup>2,5</sup>.0<sup>3,8</sup>.0<sup>4,7</sup>]octasilane. *J. Chem. Soc. Chem. Commun.* **1988**, 1083–1084. [[CrossRef](#)]
41. Furukawa, K.; Fujino, M.; Matsumoto, N. Cubic silicon cluster. *Appl. Phys. Lett.* **1992**, *60*, 2744–2745. [[CrossRef](#)]
42. Sekiguchi, A.; Yatabe, T.; Kamatani, H.; Kabuto, C.; Sakurai, H. Preparation, characterization, and crystal structures of octasilacubanes and octagermacubanes. *J. Am. Chem. Soc.* **1992**, *114*, 6260–6262. [[CrossRef](#)]
43. Matsumoto, H.; Higuchi, K.; Kyushin, S.; Goto, M. Octakis(1,1,2-trimethylpropyl)octasilacubane: Synthesis, molecular structure, and unusual properties. *Angew. Chem. Int. Ed. Engl.* **1992**, *31*, 1354–1356. [[CrossRef](#)]
44. Furukawa, K.; Fujino, M.; Matsumoto, N. Superlattice structure of octa-*tert*-butylpentacyclo[4.2.0.0<sup>2,5</sup>.0<sup>3,8</sup>.0<sup>4,7</sup>]octasilane found by reinvestigation of x-ray structure analysis. *J. Organomet. Chem.* **1996**, *515*, 37–41. [[CrossRef](#)]
45. Unno, M.; Matsumoto, T.; Mochizuki, K.; Higuchi, K.; Goto, M.; Matsumoto, H. Structure and oxidation of octakis(*tert*-butyldimethylsilyl)octasilacubane. *J. Organomet. Chem.* **2003**, *685*, 156–161. [[CrossRef](#)]
46. Sheldrick, G.M. *SADABS*; Empirical Absorption Correction Program; Institute for Inorganic Chemistry: Göttingen, Germany, 1996.
47. Sheldrick, G.M. *SHELXL-2014/7*; Program for the Refinement of Crystal Structures; University of Göttingen: Göttingen, Germany, 2014.

48. Frisch, M.J.; Trucks, G.W.; Schlegel, H.B.; Scuseria, G.E.; Robb, M.A.; Cheeseman, J.R.; Scalmani, G.; Barone, V.; Mennucci, B.; Petersson, G.A.; et al. *Gaussian 09, Revision D.01*; Gaussian, Inc.: Wallingford, CT, USA, 2009.
49. Maeda, S.; Harabuchi, Y.; Osada, Y.; Taketsugu, T.; Morokuma, K.; Ohno, K. Available online: <http://grrm.chem.tohoku.ac.jp/GRRM/> (accessed on 1 October 2018).
50. Maeda, S.; Ohno, K.; Morokuma, K. Systematic exploration of the mechanism of chemical reactions: The global reaction route mapping (GRRM) strategy using the ADDF and AFIR methods. *Phys. Chem. Chem. Phys.* **2013**, *15*, 3683–3701. [[CrossRef](#)] [[PubMed](#)]



© 2018 by the authors. Licensee MDPI, Basel, Switzerland. This article is an open access article distributed under the terms and conditions of the Creative Commons Attribution (CC BY) license (<http://creativecommons.org/licenses/by/4.0/>).